
Proceedings Paper:
Ilori, OM, Mao, X and Jaworski, AJ (2015) CFD study of oscillatory flow through 90º bends of thermoacoustic devices. In: Proceedings of ICR2015. ICR2015 : The 24th IIR International Congress of Refrigeration, 16-22 Aug 2015, Yokohama, Japan. International Institute of Refrigeration .

ID:523

CFD STUDY OF OSCILLATORY FLOW THROUGH 90º BENDS OF THERMOACOUSTIC DEVICES

Olusegun M. ILORI, Xiaoan MAO, Artur J. JAWORSKI
Faculty of Engineering, University of Leeds, Leeds LS2 9JT, United Kingdom
a.j.jaworski@leeds.ac.uk

ABSTRACT

Numerical simulation is performed to investigate oscillatory flow through 90º bends of a thermoacoustic system. Bends are often used in thermoacoustic systems as parts of acoustic networks. In the feedback loop, geometrical changes can cause system losses and it is often important to find optimal bend curvature radius that keeps the losses to the minimum. This paper investigates the effects of radius of curvature on the properties of the acoustic wave propagating through 90º bends, using 3D Computational Fluid Dynamics (CFD) simulation approach. Oscillatory flow phenomena are investigated using RANS method with SST k-ω turbulent model. Two curvature radii are considered with the drive ratio of acoustic excitation up to 0.65%. The simulation results are analysed with respect to the acoustic Dean Number and the associated flow phenomena causing losses in the bend are described. The results suggest an interesting lead that is worthy of further investigation.

1. INTRODUCTION

Bends are used in many engineering systems to achieve compactness and required changes in flow direction. In an energy system such as thermoacoustic engine and cooler, bends are used maily to form looped acoustic networks of desired configuration. Commonly used for this purpose is a 90º bend with different values of curvature radius and varying cross sectional dimensions such form (e.g. square or circular). A typical area of thermoacoustic system where bends are used is the feedback loop of a traveling wave engine which recycles acoustic wave back to the heat source for re-amplification (Yazaki et.al., 1998, and Backhaus, 2000). In such feedback loops, geometrical changes can cause system losses and it is often important to find optimal bend curvature radius that keeps the losses to a minimum in order to obtain higher limiting amplitude, which would ultimately contribute to the overall system efficiency. This type of losses is commonly referred to as minor or linear losses in the literature and mainly attributed to the viscous losses, as well as the nonlinear losses from the secondary flow that is primarily due to the dominating inertia component of the flow. The principal feature introduced by pipe curvature is a bilaterally symmetric vortical flow structure in the transverse cross-sectional plane of the pipe, caused mainly by centrifugal effects. Dean (1927, 1928) was the first to observe these flow phenomena in steady flow through curved pipe and found that the pressure drop correlates with the Dean number $\mathrm{Dn} = \mathrm{Re}\sqrt{\mathrm{d}/2\mathrm{R}}$ for a curved pipe of curvature radius R and constant cross-sectional diameter d, with the flow regime been determined by the magnitude of Reynold number, defined as $\mathrm{Re} = \mathrm{ud}/\nu$, where u and v are the average fluid velocity and kinematic viscosity, respectively. In steady pipe flow, $\mathrm{Re} \leq 2000$ denotes laminar flow with parabolic velocity profile, while the values greater than this threshold broadly represent turbulent flow.

Experimental studies have been made to characterise the extent of losses in an oscillatory flow through bends. An experimental study of oscillatory flow through coiled and straight pipes of constant circular cross-section was conducted by Oslon and Swift (1996) to investigate energy dissipation. Energy loss measurements were reported for a wide range of Reynold number and high Dean number. They measured the contribution of the entrance and exit effect of flow into the curved pipe and found it negligible compared to the energy dissipation caused by the primary and secondary flow phenomena in the curved section. Wee et al. (2012) observed in their visualisation experiment, carried out in a square cross-sectioned duct with 90º bends, that there exists a critical acoustic Dean number of 1.3 above which power loss increases drastically. They considered radius of curvature and the operating frequencies in their experiments. Numerical analysis

is important in understanding the oscillatory flow phenomena through curved geometries. An example of such study is the work of Rutten et al. (2005) that considered only laminar oscillatory flow through 90 degree bends with curvature radii one and three times the pipe diameter. Merlki and Thomann (1975) observed that the transition from laminar to turbulent oscillatory flow in a pipe occurs when the critical Reynolds number is ~400. The studies that address problem of oscillaorty flow through bends are generally limited, in comparison with the steady flow study. However, numerical study of the flow phenomena and losses associated with the oscillatory flow through the curved bends of constant circular cross section are even more difficult to find.

The current 3D CFD simulation study is performed to investigate the oscillatory flow behaviour through 90 degree bends with two different curvature radii: 1.5 and 3.6 times the pipe diameter. Time dependent flow fields are investigated with respect to these curvature radii and the ratio of mean pressure to the pressure amplitude at the antinode, refered to as the drive ratio, in the range of 0.3 to 0.65%. The simulation results are analysed with respect to normalised velocity magnitude profile and the primary and secondary flow phenomena causing losses in the 90-degree bend of thermoacoustic system.

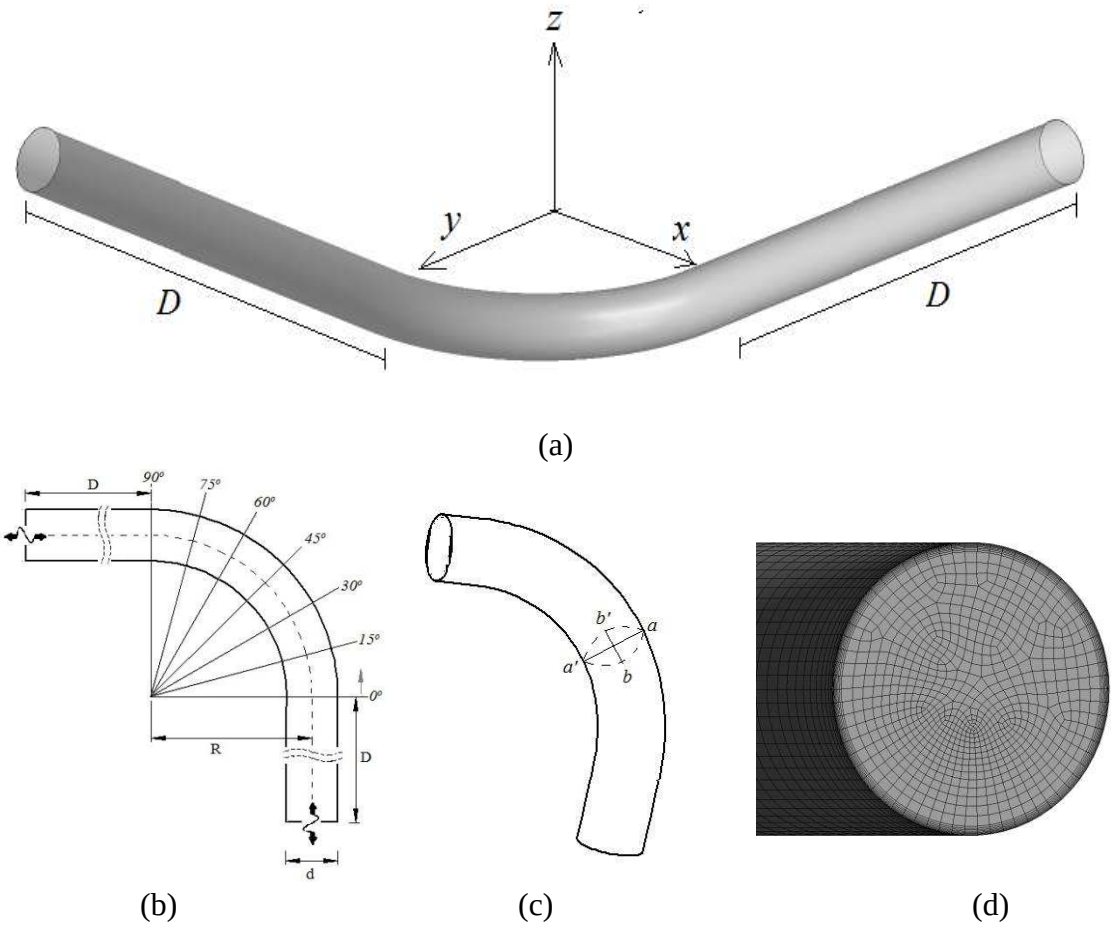

Figure 1. (a) Schematic of 90º bend section of a ½ - wavelength thermoacoustic standing wave rig, (b) definition of planes in the curved section where the flow data are obtained (c) 90º bend with plane definition, a – a' is the symmetry plane and b – b' is the perpendicular plane to the symmetry plane (d) meshed domain for the simulation study

2. NUMERICAL PROCEDURE

2.1. Geometrical model and computational domain

Figure 1a-c show the 90 degree bend and the straight section upstream and downstream of the bend with planes descriptions in the bent section. Data are taken from the symmetry and transverse planes. The

geometry consists of a 3D replica of a section of a ½-wavelength thermoacoustic standing wave rig, which forms a network of acoustic resonator where helium gas oscillates. Two 90 degree bends of different curvature radii are considered (R_1 and R_2) and represented in terms of the pipe diameter as 1.5d and 3.6d , respectively. The lengths of upstream and downstream straight section (D) are equal in dimensions and determined by the curvature radius of the 90 degree bend. For the two curvature radii, these are $12.40\,\mathrm{d}$ and $14.07\,\mathrm{d}$ respectively. In the geometry, the overall length of the entire domain remains at $30.49\,\mathrm{d}$ for any given radius of curvature.

2.2. Computational domain

The computational domain is meshed as illustrated in Fig. 1d. Fine and unstructured mesh is used in the core domain, while finer and structured mesh is used near the wall in order to accurately resolve the boundary layer where the velocity gradient is most important. The domain was chosen such that the flow structure in the curved pipe is not influenced by any unsteadiness in the oscillatory flow from the upstream and downstream sections, that is, the straight sections are long enough to ensure fully developed flow before the entrance of the curved section (Rutten et al., 2005). Inlet and outlet of the domain are defined with respect to the pressure antinode in the experimental rig. In order to characterise the required spatial discretisation and ascertain the independency of the mesh on simulation results (Rochie 1994), a systematic mesh refinement study was conducted before the actual detailed simulation study. A total volume mesh density of 189,000 was found sufficient for the simulation. However, volume mesh density of 374,400 was used in the study to further increase the accuracy of the simulation results. Geometry with radius of curvature 3.6d was used for the convergence study and subsequently same mesh count was used for the 1.5d radius of curvature. Table 1 gives the simulation parameters for the study.

Table 1. Parameters as used in the CFD simulation

Parameters	**Values/descriptions**
Medium	Helium
Mean pressure, MPa	0.1
Frequency, Hz	57
Drive ratio, %	$0.3 \le D_r \le 0.65$
Oscillation frequency, rad/s	358.142
Pipe diameter, mm	52.48

2.2.1. Characteristic parameters and governing equations

Following the traditional definition of the Dean number, the acoustic Dean number can be defined as

$$\mathrm{Dn_{ac}} = \mathrm{Re_{ac}} \cdot \sqrt{\frac{\mathrm{d}}{2\mathrm{R}}} \tag{1}$$

where $\mathrm{Re_{ac}} = \rho_o\, \mathrm{u_a}\, \mathrm{d} / \mu_o$ is the acoustic Reynolds number, with fluid density [kg/m^3], maximum velocity amplitude [m/s], hydraulic diameter [m] and the dynamic viscosity [Pa.s]. The viscous penetration depth is 0.83mm in the pipe near the wall and obtained from the following expression:

$$\delta_v = \sqrt{\frac{2\mu}{\omega \rho_m}} \tag{2}$$

where $\omega = 2\pi f$ [rad/s], ρ_m [kg/m^3], and μ [Pa.s] are the angular frequency, and mean density respectively. The simulation is carried out using Ansys Fluent 15.0. Ideal gas behaviour is assumed for the helium gas. The time dependent Reynolds Averaged Navier-stokes (RANS) equations are solved for turbulence model and are written in conservation form as:

$$\frac{\partial \rho}{\partial t} + \frac{\partial}{\partial x_j}\left(\rho u_i\right) = 0 \tag{3}$$

$$\frac{\partial(\rho u_i)}{\partial t}+\frac{\partial}{\partial x_j}\left(\rho u_i u_j\right)=-\frac{\partial p}{\partial x_i}+F_i+\frac{\partial}{\partial x_j}\left[\tau_{uj}\right]+\frac{\partial}{\partial x_j}\left(-\overline{\rho u'_i u'}_j\right)+\frac{\partial}{\partial x_i}\left(-\overline{\rho u'_i{}^2}\right)+S_m \tag{4}$$

$$\frac{\partial}{\partial t}(\rho E)+\frac{\partial}{\partial x_i}\left[u_i(\rho E+p)\right]=\frac{\partial}{\partial x_j}\left((k)_{eff}\frac{\partial T}{\partial x_j}+u_i\left(\tau_{uj}\right)_{eff}\right)+S_h \tag{5}$$

The effective stress tensor and the Reynolds Stresses term used to model momentum equation for the turbulence affected flow are given by:

$$\left(\tau_{uj}\right)_{eff}=\mu\left(\frac{\partial u_j}{\partial x_i}+\frac{\partial u_i}{\partial x_j}\right)-\frac{2}{3}\mu_{eff}\frac{\partial u_k}{\partial x_k}\delta_{ij} \tag{6}$$

$$-\overline{\rho u'_i u'}_j=\mu_t\left(\frac{\partial u_j}{\partial x_i}+\frac{\partial u_i}{\partial x_j}\right)-\frac{2}{3}\left(\rho\kappa+\mu_t\frac{\partial u_k}{\partial x_k}\right)\delta_{ij} \tag{7}$$

Equations (3) – (5) are the continuity, momentum and energy equations. SST k-ω turbulence model (Menter, 1994) is used in the simulation. SST k-omega has an advantage of resolving the flow phenomena with the boundary layer using the standard k-omega turbulence model and then switching to the k-epsilon in the region outside the boundary layer (free stream). Also, SST k-ω gave better prediction of oscillating velocity profiles near the wall and the core when compared with experimental data (Mohd Saat, 2013, Shi et al., 2010). Pressure-based solver, PISO, and second-order discretisation are used in all simulation cases.

2.2.2. Boundary and initial conditions

Pressure inlet and outlet (reversing flow) boundary conditions are specified in terms of the axial locations in the bent geometry, following analytical derivation of oscillatory variables by Swift (2001)

$$p_1(x,t)=p_o\cos(k'x_1)\cdot\cos(\omega t) \tag{8}$$

$$p_2(x,t)=p_o\cos(k'x_2)\cdot\cos(\omega t) \tag{9}$$

$$u_{a,1}=\frac{p_o}{\rho_m c}\sin(k'x_1) \tag{10}$$

$$u_{a,2}=\frac{p_o}{\rho_m c}\sin(k'x_2) \tag{11}$$

where, p_1, p_2 [Pa], $u_{a,1}$, and $u_{a,2}$ [m/s], are the pressure and velocity amplitudes at inlet and outlet of the domain (Fig. 1). $p_o = p_m D_r$ [Pa], $k'=\omega/c$ [m^{-1}], c [m/s], are the pressure amplitude at the antinode, wavenumber, and sound speed. Subscript 'm' denotes mean values. Condition (12) is set at the inlet/outlet boundaries as turbulence boundary conditions given in terms of intensity and the hydraulic diameter.

$$I=\frac{u}{U}=0.16\left(Re_a\right)^{-\frac{1}{8}} \tag{12}$$

$Re_a=\rho_o u_{a|1,2} d/\mu_o$ is the Reynolds number based on hydraulic diameter. The velocity is calculated from eq. (10) and eq. (11) for the inlet and outlet boundaries, respectively. Provided the domain is sufficiently long, this approach gave solution with an excellent match to the experimental results. The resonator wall is modelled as adiabatic and non-slip boundary conditions are applied. Time step of $\pi/250\omega$ was found to be sufficient for the convergence criteria for the transport and energy equations (10^{-5}, 10^{-5}, and 10^{-8}). Twenty five time steps make a phase in the flow cycle result into 20 phases per flow cycle. The mass flow rate through the domain was also monitored at the domain outlet to further establish the convergence of the solution and data were collected when the mass flow rate amplitude became invariant. The normalised

velocity amplitudes and axes are defined as x/d, y/d and $U = u/u_i$, where x [mm] and y [mm] are the axial location on the plane of symmetry and the plane perpendicular to the plane of symmetry respectively.

3. SIMULATION RESULTS AND DISCUSSION

3.1. CFD Code Validation

In CFD study, the principal sources of error are from the discretisation and convergence of the iterative process. The quality of boundary conditions also contributes to the accuracy of the simulation result. The validation approach employed in Ilori et al. (2014) was adopted in this study. The validation was done by comparing the analytical solution for a laminar oscillatory flow in a circular duct (Swift, 2001), with the oscillatory flow in the upstream straight section before the entrance to the curved section of the geometry with 3.6d radius of curvature. The axial velocity in the straight section was studied using the boundary conditions given in the section above and a good match was obtained in comparison with the analytical solution. Figure 2 gives the definition of the flow directions and phase (ϕ) in the acoustic cycle for velocity, pressure, and displacement amplitudes.

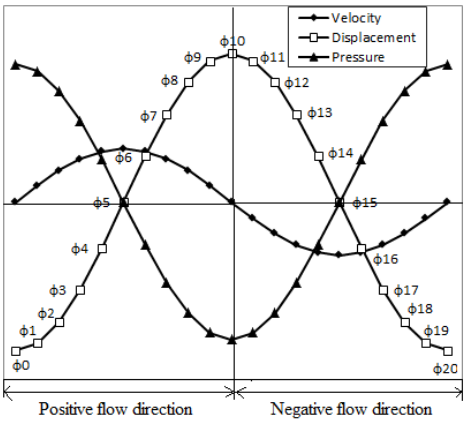

Figure 2: Definition of flow direction and the relationship between the pressure, velocity and gas displacement amplitudes

3.2. Velocity profile with directional magnitude

The results presented here are taken at planes described in Fig. 1. There are two principal planes involved – the symmetry and the perpendicular planes. Only the bend is considered and the planes are from the cross-section of the bend curvature at 0, 15, 30, 45, 60, 75 and 90 degrees, with 0 and 90 degrees representing the entrance and exit of the 90-degree bend. The choice of defining the planes with 15-degree incremental step through the bend is basically to determine the extent of influence of the curvature on the flow development at reasonable number of locations through the bend. The result is reported for the first half of the flow cycle, which corresponds to the positive flow direction as depicted in Fig. 2. To investigate the effect of curvature radius on the flow distribution, two different curvature radii are used in the study. Fluid flow characteristics are related to changes in the velocity profiles in the planes through the bend. Figure 3 shows the effects of curvature radius on velocity profiles within the bend at all the drive ratios (0.3 – 0.65%). Plotted is the velocity magnitude on the plane of symmetry (a-a') and the perpendicular (b-b') from 0 – 90-degrees for phase five (ϕ5) in the acoustic flow cycle. The velocity profiles are normalised by the maximum velocity amplitude on plane-0 and the Dean number is calculated using the maximum velocity amplitude at this location. Generally, the velocity profile is skewed towards the inner wall of the pipe for the flow in the plane of symmetry for both radii of curvature (R_1 and R_2) at the investigated drive ratios. However, the skewness is more pronounced in the case of R_1 (R = 1.5d) than that of R_2 (R = 3.6d), that is, the bend with longer curvature radius gives lower skewness in the normalised velocity profile. Furthermore, there is change in the flow behaviour between planes 15^o to 75^o for both curvature radii and at the two drive ratios. The velocity at the inner wall increased as the flow propagates through the bend. This change can be attributed to the change in the strength between the inertia and the centrifugal forces that are acting on the flow as it is developing. The normalised velocity magnitude profile in the transverse plane is shown to have almost plane wave profile at 0.3% for the both R_1 and R_2. There is a reduction in the velocity between planes 15 – 90^o for the curvature radius R_2.

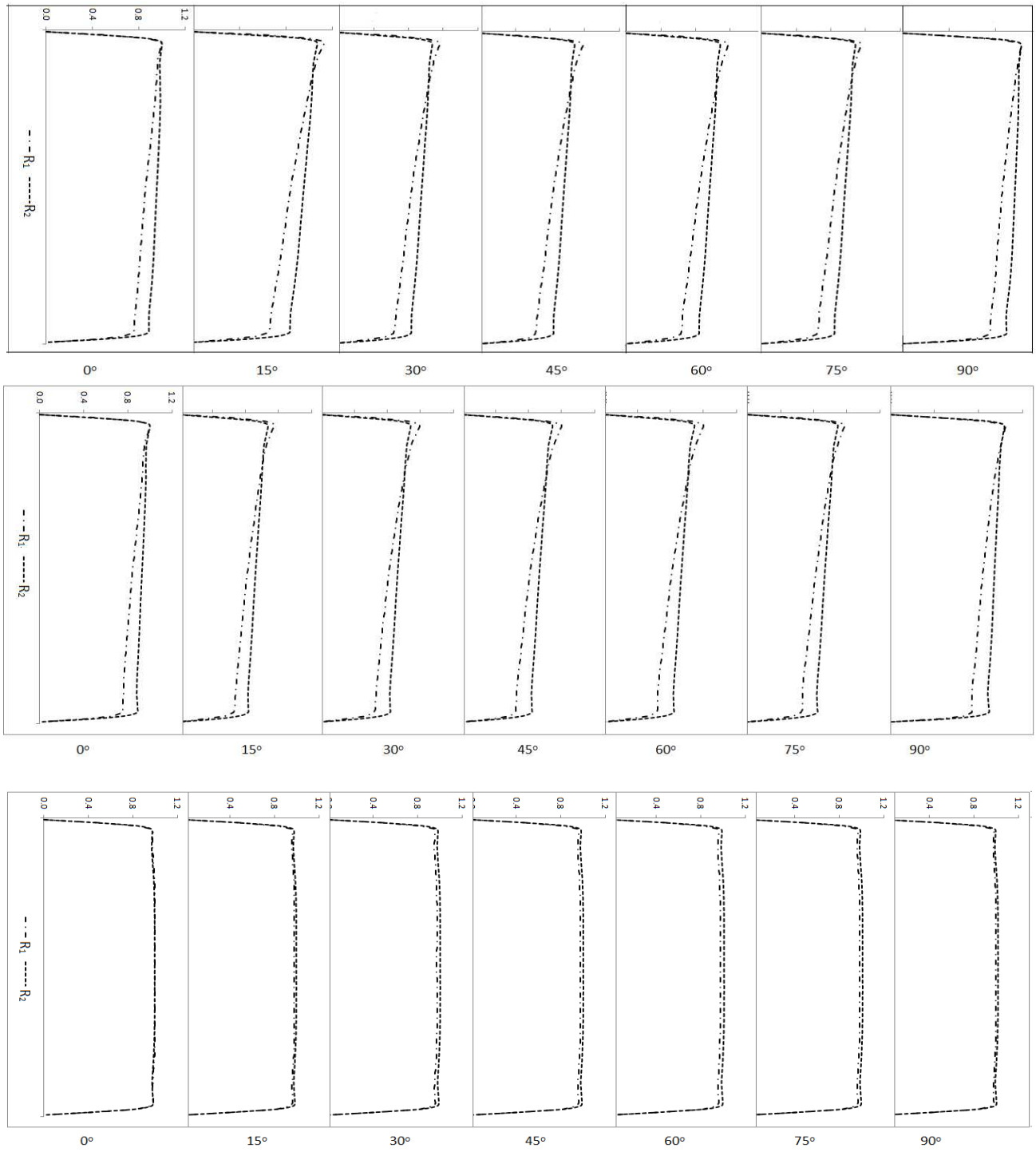

Figure 3. Oscillatory flow velocity profile along plane of symmetry in the 90-degree elbow at 0.3% drive ratio (top). Velocity profile along plane of symmetry in the 90-degree elbow at 0.65% drive ratio (middle). Velocity profile in the perpendicular plane (transverse plane) at 0.3% drive ratio (bottom).

3.3. Evolution of secondary flow

Figure 4 gives the evolution of secondary flow within the pipe bend for both curvature radii (R_1 and R_2) at drive ratio of 0.3%. Only the result for phase 5 within the acoustic flow cycle is presented in order to explain the effect that secondary flow has on losses caused by the bends in thermoacoustic system. Each of the figures depicts secondary flow as it evolves in the planes at 0º, 30º, 60º and 90º along the bend. The vector plot is based on the velocity magnitude and is normalised to give clearer representation of the flow fields. It

can be observed that the strength of secondary flow generally appears weak for the drive ratios that are considered in this study. The secondary flow structure has mainly one dominant cell with sign of gradual development into two cells at plane 60º for R_1 and at all planes of R_2 except plane 0º. This is almost as if the commonly observed twin cells in the secondary flow converged to the centre of the section. This is more visible in the bend with curvature R_1. It appears as if the oscillatory flow is dominant over the stationary component which then induces a depression in the cross-section centre thus generating a 'siphon' phenomenon characterised by sucking up the flow towards the section centre and thus forming a single secondary flow vortex. The twin vortex pair that is commonly found in the literature is yet to fully appear for the drive ratio of 0.3%. Further analysis of higher drive ratio greater than 0.3% may give an insight to the secondary flow phenomenon as relevant to the study of thermoacoustic system.

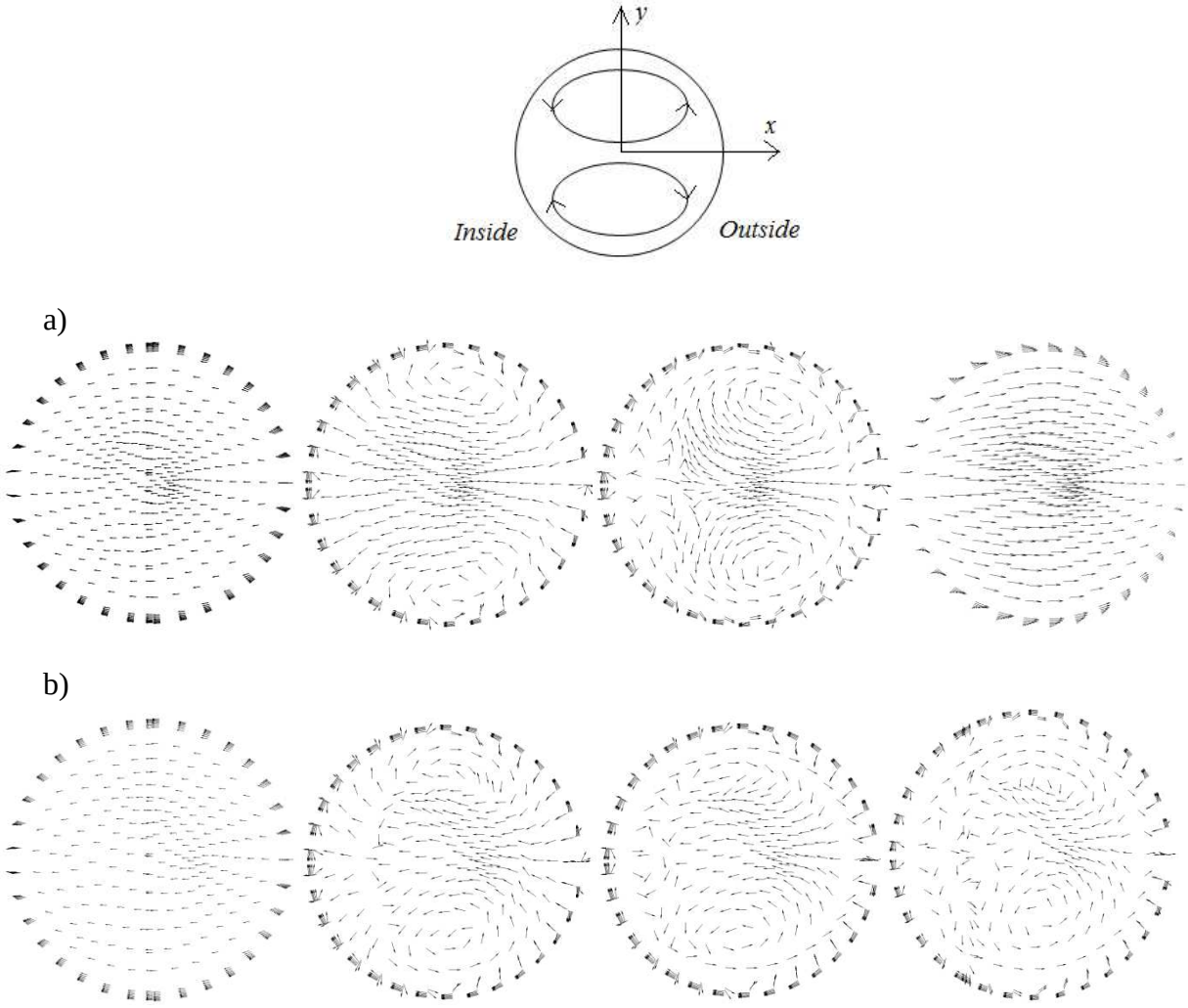

Figure 4: Development of secondary flow (velocity vectors) in the bend at drive ratio 0.3% at 0º, 30º, 60º and 90º planes along the bend (a) R_1 and (b) R_2.

4. CONCLUSION

Three-dimensional CFD simulations of oscillatory flow in a 90 degree pipe bend have been carried out in an attempt to understand the phenomena that relate to the losses caused by the curvature of bends. The effects of curvature radius on oscillatory flow were examined with respect to the drive ratios. It is observed that there is a fluid flow variation, specifically the normalised velocity profile, as a function of curvature radius of the bend. This profile skewness can be minimised when pipe bend with sufficiently long curvature is used. The results suggest the possible role of bend curvature on losses but further analysis will be required for more conclusive remark, especially on the role of secondary flow as a result of the curvature as related to losses

relevant to thermoacoustic system. Future work will consider the role of inertia and centrifugal forces on the behaviour of the flow as it propagates through the 90º bend and what loses effect are present.

ACKNOWLEDGEMENTS

Olusegun M. Ilori acknowledges the financial support from the Petroleum Technology Development Fund (PTDF), Nigeria, under the award number PTDF/E/OSS/PHD/IMO/395/11. Artur J. Jaworski would like to acknowledge the Royal Society for the support under Royal Society Industry Fellowship Scheme. This work was undertaken on ARC2, part of the HPC facilities at the University of Leeds.

REFERENCES

ANSYS Fluent 14.5.7, 2013, "User Manual," ANSYS Inc.

Backhaus S. and swift G.W., 2000, A thermoacoustic-Sterling heat engine: Detailed study, J. Acoust. Soc. Am., Vol. 107, No. 6, Pg: 3148 - 3166

Dean, W.R., 1927, Note on the motion of fluid in a curved pipe, The London, Edinburgh, and Dublin Philosophical Magazine and Journal of Science, Series 7, 4:20, 208-223

Dean, W.R., 1928, The streamline motion of fluid in a curved pipe (Second paper). The London, Edinburgh, and Dublin Philosophical Magazine and Journal of Science: Series 7, 5:30, 673-695

Ilori, O.M, Mao, X., Jaworski, A.J. 2014, CFD-Simulation of Oscillatory Flow Around the Heat Exchangers of Thermoacoustic Devices, Proc. of the ASME 2014 International Mechanical Engineering Congress & Exposition: IMECE2014-37926.

Jaworski, A. J., Mao, X., Mao X., and Yu, Z. 2009, Entrance Effects in the Channels of the Parallel Plate Stack in Oscillatory Flow Conditions, Experimental Thermal and Fluid Science, 33(3): 495-502.

Marx, D., Bailliet, H., and Valiere, J. 2008, "Analysis of the Acoustic Flow at an Abrupt Change in Section of an Acoustic Waveguide Using Particle Image Velocimetry and Proper Orthogonal Decomposition," Acta Acustica United with Acustica, 94(4): 54 – 65.

Menter, F. R. 1994, Two-Equation Eddy-Viscosity Turbulence Models For Engineering Applications, AIAA Journal, 32(8): 1598-1605.

Merlki P., and Thomann, H., 1975, Transition in Oscillating Pipe Flow, Fluid Mech., 68(3): 567-575.

Morris, P.J., Boluriaan, S., and Shieh, V.M. 2004, Numerical Simulation of Minor Losses Due to a Sudden Contraction and Expansion in High Amplitude Acoustic Resonators, ACTA Acoustica United with Acustica, 90: 393-409.

Olson, J. R. and Swift, G. W. 1996, Energy dissipation in oscillating flow through straight and coiled pipes. J. Acoust. Soc. Am. 100 (4), pg. 2123 – 2131

Roache, P. J. 1994, Perspective: A Method for Uniform Reporting of Grid Refinement Studies, Transactions-American Society of Mechanical Engineers, Journal of Fluids Engineering, 16: 405-405.

Rutten F., Schroder W., and Meinke, M., 2005, Large-eddy Simulation of Low Frequency Oscillations of the Dean Vortices in Turbulent Pipe Bend Flows.

Smith, B. L, and Swift, G. W. 2003, Power Dissipation and Time-Averaged Pressure in Oscillating Flow Through a Sudden Area Change, J. Acoust. Soc. Am. 113 (5): 2455-2463

Swift, G. W. 2001, "Thermoacoustics: A Unifying Perspective for Some Engines and Refrigerators," Los Alamos National Laboratory, (Fifth Draft, LA-UR 99-895).

Tamite B, Castelain C and Peerhossaini H., 2010, Pulsatile viscous flow in a curved pipe: Effect of pulsation on the development of secondary flow, international journal of Heat and Fluid Flow 31, pg. 879 - 896

Versteeg, K., and Malalasekera, W. 2007, An Introduction to Computational Fluid Dynamics: The Finite Volume Method, 2nd edition, England: Pearson Education Limited, Chap. 3.

Wee, S.T., Hann D.B., Abakr, Y.A. and Riley, P. 2012, PIV Wave Propagation Investigation of Non-Linear Losses through 90 Degree Bends in a Thermoacoustic Engine's Feedback Loop. AIP Conf. Proc. 1440, 1092 – 1098.

Yazaki, T., Iwata, A., Maekawa, T., and Tominaga, A., 1998, Traveling Wave Thermoacoustic Engine in a Looped Tube, Phys. Rev. Lett. 81 (15): 3128 – 3131

Yeo, R.W., Wood, P.E., and Hrymak, A.N. 1991, A Numerical Study of Laminar 90-Degree Bend Duct Flow With Different Discretization Schemes, Journal of Fluid engineering, Vol. 113 (4). Pg 563 – 568

Zhao T. and Cheng P. 1995, A Numerical Solution of Laminar Forced Convection In a Heated Pipe Subjected to a Reciprocating Flow, Int. J. Heat Mass Transfer, 38(16): 3011-3022.